CONCRETE SHIELDING ACTIVATION FOR PROTON THERAPY SYSTEMS USING BDSIM AND FISPACT-II

E. Ramoisiaux, C. Hernalsteens[1], R. Tesse, E. Gnacadja, N. Pauly, M. Vanwelde,
Service de Métrologie Nucléaire, Université libre de Bruxelles, Brussels, Belgium
F. Stichelbaut, Ion Beam Applications (IBA), Louvain-la-Neuve, Belgium
[1]also at CERN, Geneva, Switzerland

Abstract

Proton therapy systems are used worldwide for patient treatment and fundamental research. The generation of secondary particles when the beam interacts with the beamline elements is a well known issue. In particular, the energy degrader is the dominant source of secondary radiation. This poses new challenges for the concrete shielding of compact systems and beamline elements activation computation. We use a novel methodology to seamlessly simulate all the processes relevant to the activation evaluation. A realistic model of the system is developed using Beam Delivery Simulation (BDSIM), a Geant4-based particle tracking code that allows a single model to simulate primary and secondary particle tracking and all particle-matter interactions. The secondary particle fluxes extracted from the simulations are provided as input to FISPACT-II to compute the activation by solving the rate equations. This approach is applied to the Ion Beam Applications (IBA) Proteus®ONE (P1) system and the shielding of the proton therapy research centre of Charleroi, Belgium. Proton loss distributions are used to model the production of secondary neutrals inside the accelerator structure. Two models for the distribution of proton losses are compared for the computation of the clearance index at specific locations of the design. Results show that the variation in the accelerator loss models can be characterised as a systematic error.

INTRODUCTION

Numerous proton therapy centres have been built for patient treatment and fundamental research over the past two decades [1]. It is well known that proton therapy machines generate a large number of secondary particles, mainly neutrons, when the proton beam interacts with the beamline elements [2]. In particular, the energy degrader is the dominant source of secondary radiation. Those neutrons interact with the concrete shielding via nuclear reactions, mainly neutron capture and spallation, producing radioactive nuclides. Some are long-lived and are responsible for the long-term activation of the shielding.

When designing a new centre or preparing experimental setups, the complete modelling of proton therapy systems from the primary and secondary beam interactions to the beamline and shielding activation is a complex but necessary task. We establish a method, inspired from the Rigorous Two-Step (R2S) [3], coupling Beam Delivery SIMulation (BDSIM) [4] with the code and library database FISPACT-II [5]. BDSIM provides a full 3D model of the proton therapy system and its shielding that includes the particle-matter interactions of Geant4 and the tracking of all the particles through the beamline magnetic elements, vacuum windows and air gaps. FISPACT-II is subsequently used for the activation computation.

This methodology is thoroughly described in Ref. [6] and was applied to the shielding design of the future proton therapy centre of Charleroi, Belgium. The IBA Proteus®ONE proton therapy system that will be used in the centre was already modelled in BDSIM and validated against experimental data in Ref. [7]. The model was then used for the secondary particle generation required for shielding activation studies with FISPACT-II. The shielding activation results were fully validated against the IBA shielding design that was obtained using MCNPX [8].

During the elaboration of the BDSIM model of the future proton therapy centre of Charleroi, it was required to model in detail the proton loss pattern inside the accelerator (S2C2). Indeed, the acceleration of the primary protons is not simulated in BDSIM and therefore, the secondary neutron generation is realised by combining two different simulations. The first simulation considers the transport of the primary particles through the beamline with the secondary neutrons generated by interactions of the beam with the beamline elements. On the other hand, the second simulation simulates the propagation of lost protons inside the S2C2 structure. The S2C2 secondary neutrons generation process is presented in Fig. 1.
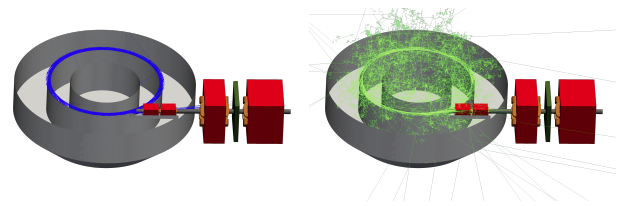

Figure 1: Illustration of the S2C2 secondary neutrons generation process in BDSIM. The protons (shown in blue) and the neutral particles, neutrons and photons (shown in green) are represented. Distribution of protons lost during the acceleration and the extraction processes serve as primary input (left). The resulting secondaries are produced by the interactions of the protons with the S2C2 structure (right).

We propose to use the BDSIM/FISPACT-II methodology to characterise the impact of two S2C2 proton loss distributions on the activation results. Figure 2 represents the BDSIM model of the vault of the proton therapy centre of Charleroi with its concrete shielding design. The concrete shielding was implemented using *Pyg4ometry*, a Python library that enables users to create GDML-based geometry rapidly [9, 10]. The S2C2 and the degrader, the two main elements of the beamline at the origin of most of the secondary particle generation, can be observed. We study the activation

MC6: Beam Instrumentation, Controls, Feedback and Operational Aspects

T18: Radiation Monitoring and Safety

This is a preprint — the final version is published with IOP

inside a cylindrical volume in the North Wall as it is the wall most affected by the S2C2 secondary neutrons. The specific location and geometry of the volume have been chosen to fit with a possible future experimental measurements campaign design that will consist of cylindrical removable concrete cores placed in the most irradiated parts of the shielding vault.
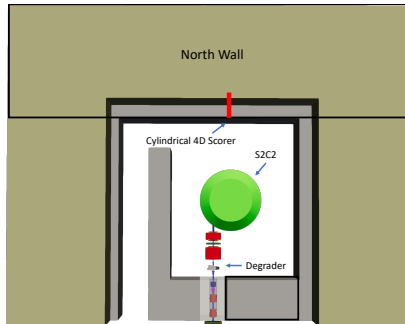

Figure 2: Realistic model of the S2C2 vault shielding. The North Wall is designated as well as the cylindrical mesh position.

The activity of a compound is determined by its clearance index. The clearance index is defined as the sum A_i/CL_i over all the material radionuclides with A the specific activity and CL the clearance level allowed by the Belgian legislation. If the clearance index exceeds the value of 1, the compound is considered radioactive waste. The main isotopes produced in concrete are listed in Table 1 with their corresponding clearance level.

Table 1: Clearance Levels for the Main Isotopes Produced in Concrete [11]

Nuclide	CL (Bq/g)	Nuclide	CL (Bq/g)
^{3}H	100	^{60}Co	0.1
^{7}Be	10	^{134}Cs	0.1
^{22}Na	0.1	^{152}Eu	0.1
^{54}Mn	0.1	^{154}Eu	0.1

TOOLS AND METHODS

Simulations with two different proton loss distributions inside the S2C2 have been realised using the BDSIM model. The irradiation condition studied are those used during the centre dimensioning [6]: 300 hours of irradiations per year with an S2C2 current of 150 nA. The degrader has been calibrated for a delivered beam energy of 100 MeV, which is the future centre most-used value.

The two distributions for the S2C2 losses were characterised based on the IBA design [11]. For both loss models, we consider that 25 % of the beam current is lost uniformly along the circumference at top energy (230 MeV) and that 45 % of the beam current is lost at the septum level during the extraction phase, as shown in Fig. 3.

In the first S2C2 loss model, model A, all the proton losses are simulated in the horizontal mid-plane, with the septum loss emitted in the forward direction. In the second model,
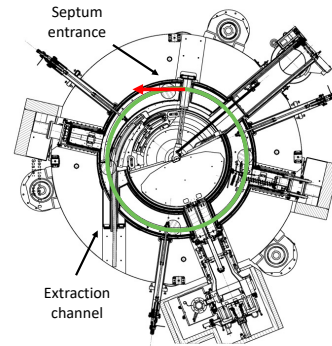

Figure 3: Illustration of the two sources of proton losses in the S2C2 simulated in BDSIM: the uniformly distributed losses along the accelerator circumference (in green) and the losses located at the septum (in red).

model B, a normally distributed contribution of 1 mm (resp. 1 mrad) σ is added to the vertical position (resp. direction) of the circumference lost protons, while the septum lost protons are uniformly distributed in a 30° cone. The two S2C2 loss models are represented in Fig. 4.
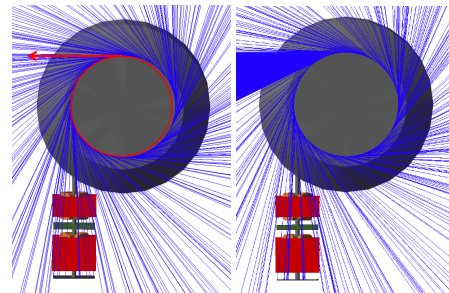

Figure 4: S2C2 loss models. On the left, model A, with the circumference losses simulated in the horizontal mid-plane and the septum losses emitted along with the red arrow. On the right, model B, with a normally distributed contribution of 1 mm (resp. 1 mrad) σ added to the vertical position (resp. direction) of the circumference lost protons and the septum loss uniformly distributed in a 30° cone.

The differential fluence of the secondary neutrons is scored following the predefined energy group structure "CCFE-709" in the cylindrical scorer mesh presented in Fig. 2 using the 4D-Scoring BDSIM feature [12]. The comparison between the neutron differential fluence in the cylindrical core when using either of the models is presented in Fig. 5. The differential secondary fluences obtained from the circumference losses are almost identical between the two models. This similarity is expected behaviour as the impact of the random variation in position and angle of the lost protons simulated for the circumference losses is entirely hidden by the multiple scattering and interactions that the protons undergo inside the S2C2 structure. On the other hand, the differential fluence obtained from the septum losses is higher when using model A. This difference is easily explained by the variation of the septum losses distributions in model B, which spreads the secondary neutrons away from the North wall.
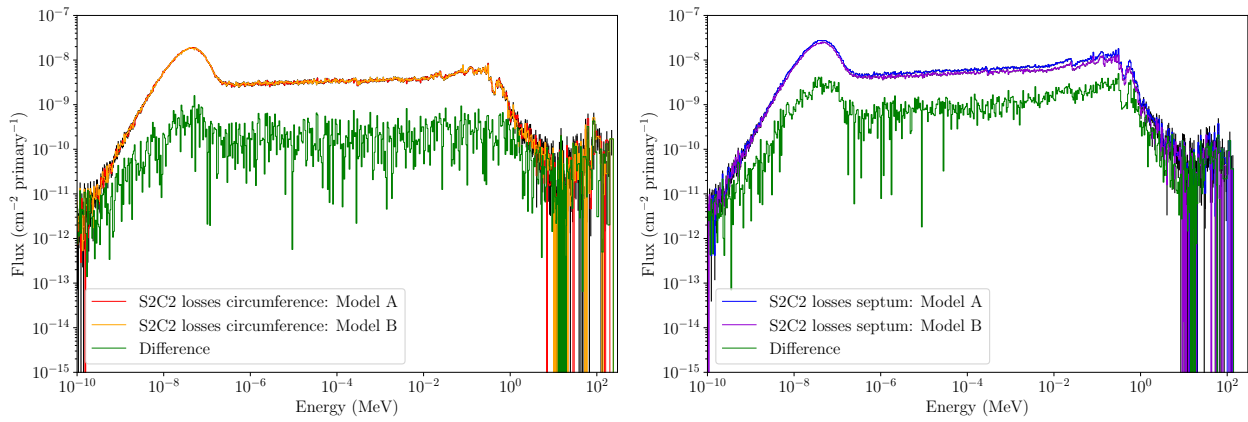
Figure 5: Comparison of the differential secondary neutron fluence extracted from the first 10 cm of the scored volume using the BDSIM 4D Scoring feature between the two S2C2 models. The differential secondary neutron fluence generated from the S2C2 circumference losses on the left and from the septum on the right.

The differential fluences of the secondary neutrons are then provided to FISPACT-II to compute the activation over an irradiation and a cooling period of 20 years. The clearance index is calculated along the cylindrical scored volume for both S2C2 loss models and the beamline losses. In Fig. 6, the activation associated with model A is observed to be larger than for model B, as expected by the comparison of the related differential fluences distributions. The most substantial difference between the models is 7 %. These results are not critical as the activated thickness - the depth at which the clearance index drops below 1 - is not impacted.
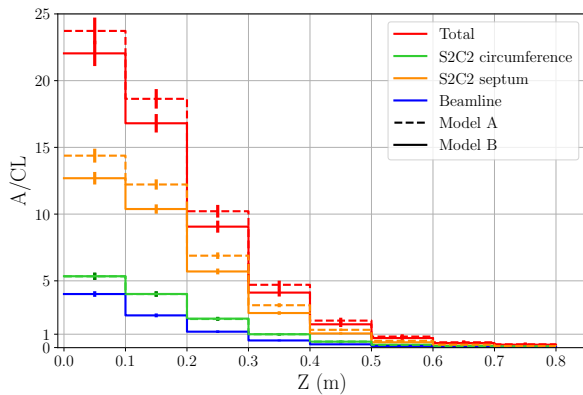

Figure 6: Evolution of the clearance index along with the thickness of the scored volume. The clearance indexes related to the circumference and the septum S2C2 losses are represented in green and orange, to the beamline losses in blue, and the total is represented in red.

FISPACT-II computation results also provide information about the impact of either model on the evolution of the radioactive nuclides concentration in the scored volume. The evolution of the clearance index of the most radioactive part of the core following the main radioactive nuclides is presented in Fig. 7. The nuclide-related activation varies only slightly between models A and B. Such variation will not significantly impact experimental measurements of the activation. The variation in the S2C2 loss models can be characterised as a systematic error.
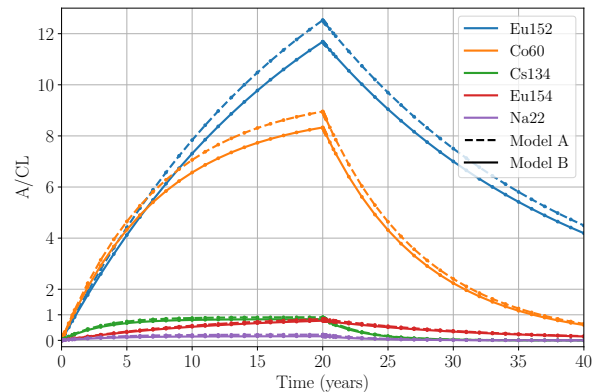

Figure 7: Evolution of the clearance index of the most radioactive part of the core following the main radioactive nuclides.

CONCLUSION AND OUTLOOKS

The BDSIM/FISPACT-II methodology has been applied to the specific case of determining if the choice of the S2C2 loss patterns impacts the activation results. The activation along a cylindrical scorer in the North Wall of the vault was studied. The results compared the two models and showed a minimal variation for the activation after 20 years of operation and its evolution per nuclides. This variation between models can therefore be characterised as a systematic error. Such models of the S2C2 loss patterns will be used for further studies without impacting their main results.

ACKNOWLEDGMENT

This is a preprint — the final version is published with IOP

REFERENCES

[1] PTCOG. (2021) Particle therapy co-operative group - particle therapy centers. https://www.ptcog.ch/.

[2] H. Paganetti, *Proton Therapy Physics*, CRC Press, MGH and HMS, Boston, USA, 2011.

[3] Y. Chen and U. Fischer, "Rigorous mcnp based shutdown dose rate calculations: computational scheme, verification calculations and application to ITER," *Fusion Eng. Des.*, vol. 63-64, pp. 107–114, Dec. 2002. doi:10.1016/S0920-3796(02)00144-8

[4] L. J. Nevay *et al.*, "BDSIM: An accelerator tracking code with particle-matter interactions," *Comput. Phys. Commun*, vol. 252, p. 107200, 2020. doi:10.48550/arXiv.1808.10745

[5] J.-C. Sublet *et al.*, "FISPACT-II: An advanced simulation system for activation, transmutation and material modelling," *Nucl. Data Sheets*, vol. 139, pp. 77–137, 2017. doi:10.1016/j.nds.2017.01.002

[6] E. Ramoisiaux *et al.*, "Self-consistent numerical evaluation of concrete shielding activation for proton therapy systems," *Eur. Phys. J. Plus*, 2022, submitted for publication.

[7] C. Hernalsteens *et al.*, "A novel approach to seamless simulations of compact hadron therapy systems for self-consistent evaluation of dosimetric and radiation protection quantities," *EPL*, vol. 132, p. 50004, 2021. doi:10.1209/0295-5075/132/50004

[8] D. Pelowitz, *MCNPX 2.6 Manual*, Los Alamos National Laboratory, 2008.

[9] S. T. Boogert *et al.*, "Pyg4ometry : A Tool to Create Geometries for Geant4, BDSIM, G4Beamline and FLUKA for Particle Loss and Energy Deposit Studies", in *Proc. IPAC'19*, Melbourne, Australia, May 2019, pp. 3244–3247. doi:10.18429/JACoW-IPAC2019-WEPTS054

[10] S. Walker *et al.*, "Pyg4ometry: A python library for the creation of monte carlo radiation transport physical geometries," *Comput. Phys. Commun*, vol. 272, p. 108228, 2022. doi:10.1016/j.cpc.2021.108228

[11] F. Stichelbaut, IBA, Tech. Rep., 2019.

[12] E. Ramoisiaux *et al.*, "BDSIM Developments for Hadron Therapy Centre Applications", in *Proc. IPAC'21*, Campinas, Brazil, May 2021, pp. 1252–1255. doi:10.18429/JACoW-IPAC2021-MOPAB416